Superconductor Science and Technology

LETTER • **OPEN ACCESS**

Record field in a 10 mm-period bulk high-temperature superconducting undulator

To cite this article: Kai Zhang *et al* 2023 *Supercond. Sci. Technol.* **36** 05LT01

OPEN ACCESS
IOP Publishing

Letters
Superconductor Science and Technology

Supercond. Sci. Technol. **36** (2023) 05LT01 (7pp)
https://doi.org/10.1088/1361-6668/acc1a8

Letter

Record field in a 10 mm-period bulk high-temperature superconducting undulator

Kai Zhang[1,7], Andrew Pirotta[1,2], Xiaoyang Liang[1,3], Sebastian Hellmann[1], Marek Bartkowiak[4], Thomas Schmidt[1], Anthony Dennis[5], Mark Ainslie[6], John Durrell[5] and Marco Calvi[1,*]

[1] Insertion Device Group, Photon Science Division, Paul Scherrer Institute, Villigen 5232, Switzerland
[2] Department of Microelectronics and Nanoelectronics, University of Malta, Msida, Malta
[3] Institute of Biomedical Engineering, ETH Zürich, 8092 Zürich, Switzerland
[4] Sample Environment Group, Neutrons and Muons Division, Paul Scherrer Institute, Villigen 5232, Switzerland
[5] Bulk Superconductivity Group, Department of Engineering, University of Cambridge, Cambridge CB2 1PZ, United Kingdom
[6] Department of Engineering, King's College London, Strand, London WC2R 2LS, United Kingdom
[7] Now with Zhangjiang Laboratory, Shanghai 201210, People's Republic of China

E-mail: marco.calvi@psi.ch

Received 28 November 2022, revised 16 February 2023
Accepted for publication 6 March 2023
Published 15 March 2023

Abstract

A 10 mm-period, high-temperature superconducting (HTS) undulator consisting of 20 staggered-array $GdBa_2Cu_3O_{7-x}$ (GdBCO) bulk superconductors has been fabricated and tested successfully. Each GdBCO disk was machined into a half-moon shape with micro-meter accuracy and shrink-fitted into a slotted oxygen-free copper disk which provided pre-stress and effective conduction-cooling. The HTS undulator prototype, consisting of GdBCO disks, copper disks, and CoFe poles fitted in a long copper shell, was field-cooled magnetized in fields of up to 10 T at 10 K. An undulator field of 2.1 T in a 4 mm magnetic gap was obtained. This field is the largest reported yet for the same gap and period length and exceeds the target value of 2 T for the meter-long HTS undulator scheduled for the hard x-ray I-TOMCAT beamline in the Swiss Light Source 2.0. We have demonstrated that bulk superconductor based undulators can provide significantly improved performance over alternative technologies.

Keywords: HTS, superconducting undulator, short period, magnetization, FEL

(Some figures may appear in colour only in the online journal)

* Author to whom any correspondence should be addressed.

1. Introduction

Superconducting undulators (SCUs) exhibit excellent tunability of radiation wavelength and durable operation without demagnetization induced by electron beam losses. SCUs have been successfully developed and commissioned for user operation in the Karlsruhe Institute of Technology synchrotron and the Advanced Photon Source (APS) storage ring in the past decade [1–3]. Compared to permanent magnet undulators (PMUs) [4], SCUs provide unparalleled photon flux in the high energy part of the x-ray spectrum. However, when the undulator period, λ_u, is below 15 mm a standard NbTi SCU does not provide a higher on-axis undulator field, B_0, than the best cryogenic PMUs for the same magnetic gap, g [5]. The reduction in both λ_u and B_0 results in a low deflection parameter $K = 0.934\lambda_u[\text{cm}]B_0[\text{T}]$ below which no high harmonic photons can be effectively utilized in synchrotron light sources. Nb_3Sn conductor with higher engineering current density J_e has been selected for the development of several SCU prototypes for the APS storage ring and the Linac Coherent Light Source II [6, 7], however, its superiority has not yet been validated for a period less than 15 mm.

Short undulator prototypes consisting of high-temperature superconducting (HTS) coils have been widely studied but have not yet delivered performance superior to NbTi or Nb_3Sn undulators [8–11]. A promising approach for achieving high B_0 for a short period λ_u is to employ a staggered-array bulk HTS undulator (BHTSU) [12–14]. The BHTSU consists of a series of staggered-array $ReBa_2Cu_3O_{7-x}$ (ReBCO) bulks which are field-cooled (FC) magnetized by a superconducting solenoid. Experimental studies on 10 mm-period BHTSU prototypes demonstrate that the on-axis field B_0 can reach 0.85 T for $g = 6$ mm and 1.54 T for $g = 4$ mm, respectively [14, 15]. Importantly, these results were obtained at 10 K which could be achieved with reduced cooling cost in comparison to ~4 K required for NbTi/Nb_3Sn undulators.

In this letter, we report an undulator field of 2.1 T obtained in a BHTSU prototype made of industrial GdBCO/Ag bulks with a designed period of 10 mm and magnetic gap of 4 mm.

2. Experiments

Quenches occurred in previous short undulator prototypes made of GdBCO/Ag bulks. These were ascribed to three possible influences: (a) poor assembly which resulted in relative motion between disks during magnetization; (b) poor cooling capability due to the gaps being filled with epoxy resin and (c) large Lorentz forces and associated tensile stresses in the GdBCO/Ag bulks during magnetization. To address these issues we designed a new 10-period BHTSU prototype, as shown in figure 1. It consists of commercial GdBCO bulks from Nippon Steel Corporation and exploits the shrink-fit assembly technique which helps to constrain the GdBCO disks, provide better cooling conditions and reduce their tensile stresses [16, 17].

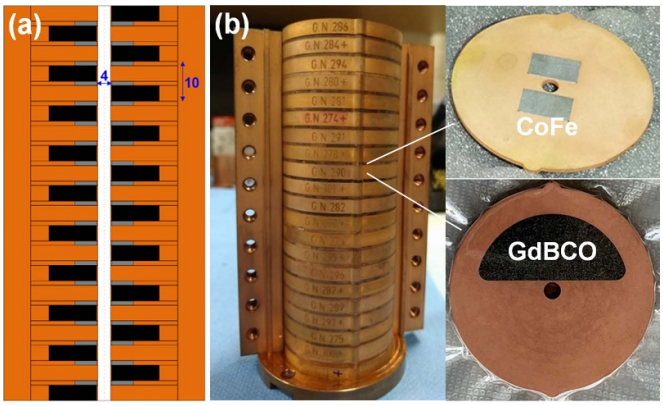

Figure 1. (a) Midsection view of the 10-period staggered-array bulk HTS undulator; (b) cutaway view of the undulator, with 20 GdBCO-Cu pieces, 19 CoFe-Cu pieces and a half copper shell shown in the figure. Each 4 mm-thick, half-moon shaped GdBCO disk is shrink-fitted into a slotted copper disk; two rectangular 1 mm-thick CoFe poles are shrink-fitted into a slotted copper disk; all GdBCO-Cu and CoFe-Cu pieces are clamped by a long copper shell. The undulator has a period length of 10 mm and magnetic gap of 4 mm.

Measured results of the mechanical strains in a previous half-period bulk YBCO undulator suggest the superconducting disk is well compressed by the copper disk after cool down to 77 K. More details about the strain measurement can be found in the appendix. To predict how much the applied prestress by the copper disk and the aluminum shell could compensate the Lorentz forces, a one-quarter 3D electromagnetic-mechanical coupled finite element analysis model was created in ANSYS to simulate the FC magnetization from 8 T with implementation of the E–J power law ($J_c = 1 \times 10^{10}$ A m^{-2}, $n = 20$) and compare the peak tensile stress in the GdBCO disk with and without being pre-stressed [18]. As shown in figure 2, during magnetization the peak 1st principal stress (maximum tensile stress) in the pre-stressed GdBCO disk reaches 39 MPa, significantly lower than the 82 MPa experienced by an unconstrained GdBCO disk. A direct comparison of the stress patterns for $\Delta B_s = 8$ T is provided on the right hand side of figure 2. It can be observed that the majority of the pre-stressed GdBCO disk experiences compressive stress which is unproblematic in ceramic-like materials, while the rest experiences only modest tensile stress.

The undulator design incorporates a period length of 10 mm, magnetic gap of 4 mm and mechanical gap of 3.4 mm. The half-moon shaped GdBCO disks, long copper shell, slotted oxygen-free copper disks and CoFe poles are machined with micro-meter accuracy utilizing electrical discharge machining wire erosion. The assembly was carried out as follows

(i) The slotted copper disks were first heated up to 200 °C;
(ii) The GdBCO disks and CoFe poles (expected to enhance the undulator field B_0 by 10%–15%) were then pressed into the copper disks;

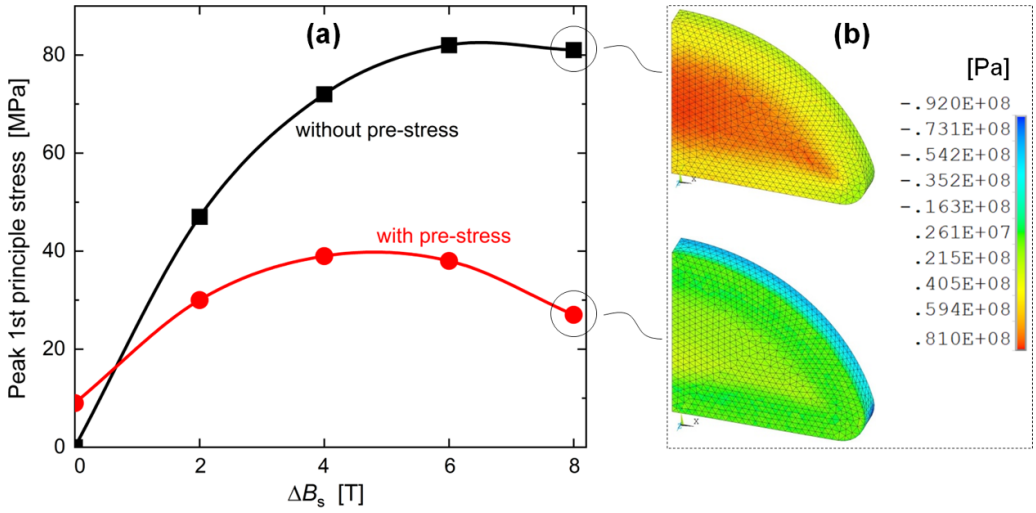

Figure 2. (a) Comparison of peak 1st principal stresses in the half-moon shaped GdBCO disk with and without pre-stress during FC magnetization from 8 T to zero; (b) 1st principal stress patterns in pre-stressed and pre-stress-free GdBCO disks for $\Delta B_s = 8$ T. These are calculated results from numerical simulations carried out in ANSYS.

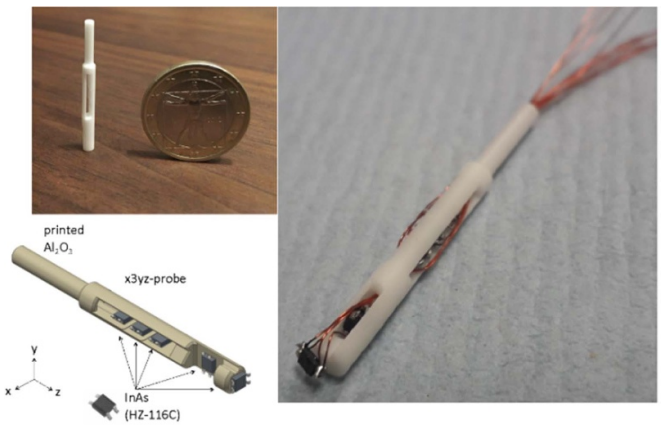

figure 3. 3D printed *x*3*yz* probe for measuring the undulator field. Images are reprinted from [5].

(iii) All GdBCO-Cu and CoFe-Cu pieces were finally clamped by a long copper shell as shown in figure 1.

After assembly, the undulator sample was connected to the vertical magnetic field measurement system and installed in a variable temperature insert in the 12 T superconducting solenoid in the Bulk Superconductivity Group at the University of Cambridge. The undulator is cooled directly by flowing helium gas and its working temperature is controlled by a heater wrapped on the outer copper shell. A 3 mm-diameter *x*3*yz*-probe shown in figure 3, supported by a meter-long carbon fiber reinforced plastic tube and controlled by a motorized linear stage outside the cryostat, is employed to characterize the on-axis magnetic field in three orthogonal directions. The undulator field B_y is measured at three different y positions, with one on-axis and the other two off-axis of ± 0.1 mm. For other details regarding the experimental setup, please refer to [14].

3. Results

The BHTSU prototype made of Nippon GdBCO bulks was first FC magnetized from 10 T to 0 T at 10 K with the on-axis field measured every 1 T and then subcooled to 7.5 K to minimize the flux creep. The field ramp rate was kept at ~ -1 T h^{-1} during magnetization. By analyzing the measured field profiles from one on-axis InAs sensor and the other two off-axis of ± 0.1 mm we observe that there is an offset of ~ 0.1 mm between the undulator axis and the axis of the 3 mm-diameter *x*3*yz*-probe. The measurement field profile with the smallest amplitude is thus considered as the practical on-axis undulator field.

Figure 4 summarizes the measured on-axis magnetic field profiles during the full FC magnetization process. Higher field amplitude was observed at both ends because the periodicity stops and the sizes of the end bulks were not optimized in this stage. To evaluate the performance under various ΔB_s, we have compared the mean undulator field B_0 (the two end peaks are excluded) and the field inhomogeneity σ_B/B_0 as shown in figure 5. σ_B is the modified standard deviation and estimated by

$$\sigma_B = \sqrt{\frac{1}{N_1+N_2}\left(\sum_{i=1}^{N_1}\left(B_i^+ - B_0^+\right)^2 + \sum_{i=1}^{N_2}\left(B_i^- - B_0^-\right)^2\right)} \quad (1)$$

where B_i^+ are the positive peaks, B_0^+ is the mean value of the positive peaks, B_i^- are the negative peaks, B_0^- is the mean value of the negative peaks, N_1 is the number of positive peaks, and N_2 is the number of negative peaks ($N_1 + N_2 = 17$). As ΔB_s increases, both the penetration depth in the GdBCO disks and associated undulator field B_0 rise. When ΔB_s is below 5 T there is a linear relation between B_0 and ΔB_s, i.e. $B_0 = a_0 + a_1 \Delta B_s$ where $a_0 = 32.4$ mT and

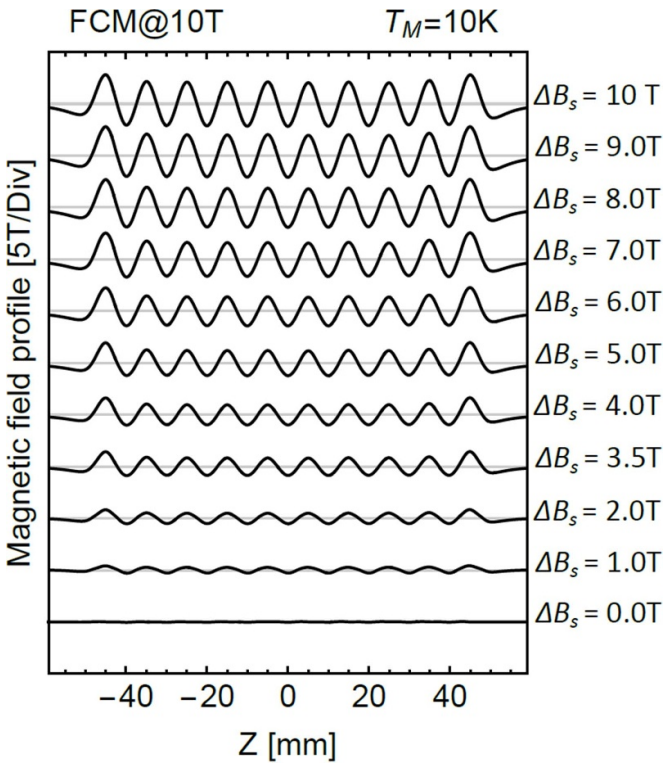

Figure 4. Measured on-axis magnetic field during the FC magnetization. ΔB_s refers to the change in the background solenoid field.

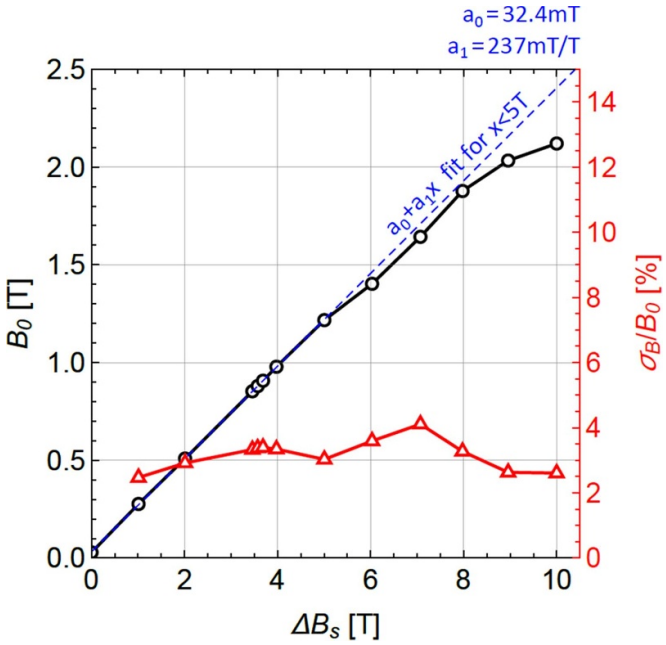

Figure 5. Relation between the mean undulator field B_0, σ_B/B_0 and ΔB_s. A record field of 2.1 T is obtained for a 10 mm-period undulator.

$a_1 = 237$ mT T^{-1}; if a small offset is neglected, this relation remains valid until 8 T where the onset of a different regime becomes visible. This is because the magnetization of the GdBCO disks is close to saturation and further penetration occurs far from the central axis. When ΔB_s rises up to 10 T, an undulator field B_0 of 2.1 T is obtained with $\sigma_B/B_0 = 2.7\%$. About 2.1 T is the largest yet reported undulator field for a period length of 10 mm and exceeds the target value of 2 T for the meter-long HTS undulator scheduled for the hard x-ray I-TOMCAT beamline in the Swiss Light Source 2.0 (SLS 2.0). By either swapping the GdBCO disks or adjusting the heights of CoFe poles, we expect that

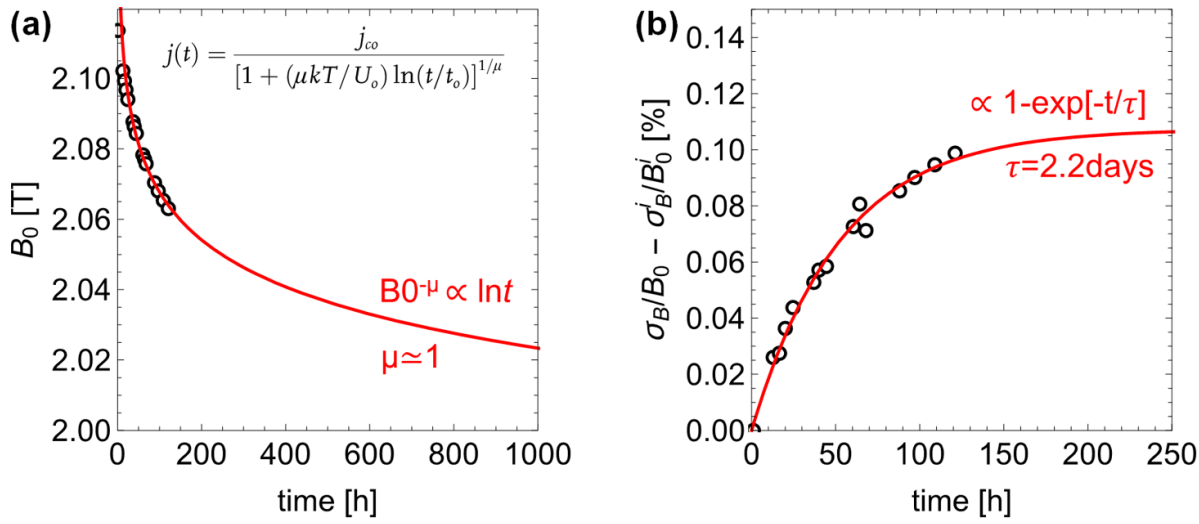

Figure 6. (a) Field decay over time due to the flux creep; (b) stabilization of the field inhomogeneity over time.

the field inhomogeneity can be further minimized and a root mean square (RMS) phase error of only a few degrees can be achieved [19].

To minimize the flux creep-induced field decay, the BHTSU prototype was subcooled to 7.5 K after FC magnetization from 10 T to zero. The undulator field was measured immediately after subcooling and during the initial field decay over 120 h. The measured data points of B_0 were fitted by the 'interpolation formula', the time dependence of the persistent current $j(t)$ in the collective creep model suggested in [20]. It is expected that $B_0^{-\mu}$ ($\mu = 1$) is proportional to ln$t$ with further increase in the waiting time as shown in figure 6(a). In the meantime, the field inhomogeneity increases over time but its change, $\sigma_B/B_0 - \sigma_B^i/B_0$, is very small and it seems to stop with an exponential trend, i.e. proportional to $1-e^{-t/\tau}$ where $\tau = 2.2$ d as shown in figure 6(b).

4. Conclusion

A HTS undulator prototype made of industrial GdBCO/Ag bulks has been fabricated with new machining and assembling techniques. We have achieved a mean B_0 of up to 2.1 T with a 10 mm-period and 4 mm-magnetic gap. This undulator field of 2.1 T is the highest achieved to date for such a short period and exceeds the target value required for the I-TOMCAT beamline in the SLS 2.0. The quenches that hindered our previous undulator prototypes have been eliminated in this experiment thanks to new undulator fabrication techniques. The field inhomogeneity caused by J_c variation among GdBCO disks is within 2.7%. It is observed that the flux creep is not negligible after subcooling from 10 K to 7.5 K while the field homogeneity reduces slightly over time.

Data availability statement

All data that support the findings of this study are included within the article (and any supplementary files).

Acknowledgments

This work was performed under the auspices and with support from the Swiss Accelerator Research and Technology (CHART) program (www.chart.ch), the LEAPS-INNOV WP6 (www.leaps-innov.eu/) and Cambridge Royce facilities grant EP/P024947/1. The work of M D Ainslie was carried out while affiliated with the Bulk Superconductivity Group, Department of Engineering, University of Cambridge, and supported by the EPSRC Early Career Fellowship, EP/P020313/1. The authors would like to acknowledge the RIKEN SPring-8 Center for the constant support to our development, specifically for the procurement of the ReBCO crystals used for the preparation of the undulator sample and to thank L A C. Huber from Paul Scherrer Institute for technical support in preparing the sample. All data are provided in full in the results section of this paper.

Appendix

To validate the shrink-fit assembly technique, we first assembled a half-period undulator prototype consisting of a 4 mm-thick, half-moon shaped YBCO disk, slotted copper disk and aluminum shell, as shown in figure 7(a). To quantify the pre-stress contributions, eight strain gauges were mounted on the YBCO disk and one strain gauge was mounted on a small stress-free YBCO block for thermal compensation, as shown in figure 7(b). An inverse measurement of the mechanical strains was carried out as follows

(i) Connect all strain gauges to 1/4 Wheatstone bridges and record the initial balance values at room temperature (RT) as S_{YCA}^{RT} (Y = YBCO disk, C = copper disk, A = aluminum shell), then immerse the YBCO-Cu-Al piece and small YBCO block into LN_2 and record the measurement values as S_{YCA}^{77K};

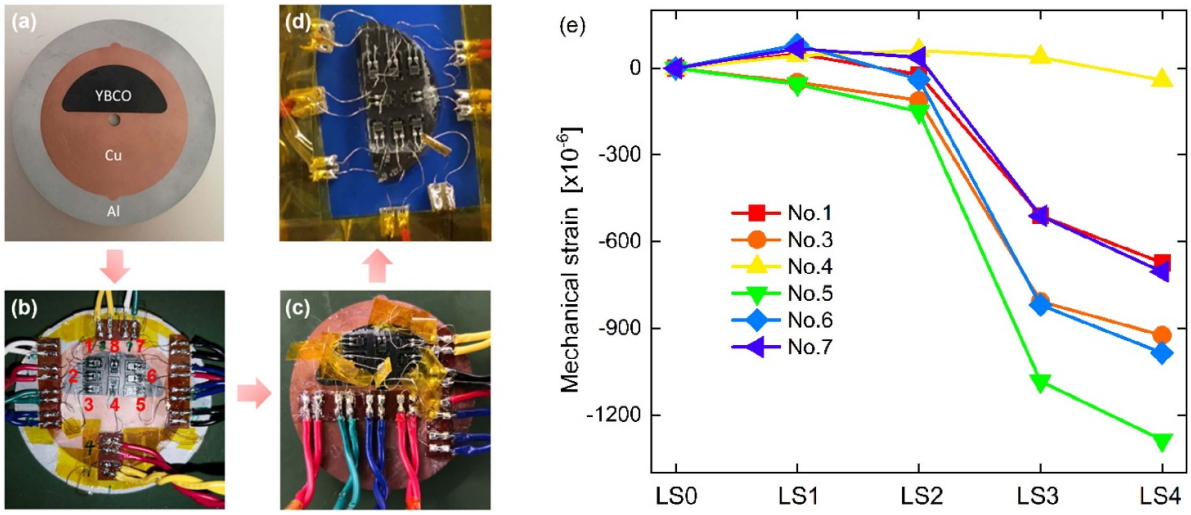

Figure 7. Inverse measurement of mechanical strains in the half-moon shaped YBCO disk. (a) Layout of the shrink-fitted, 4 mm-thick YBCO-Cu-Al piece; (b) YBCO-Cu-Al piece with mounted strain gauges; (c) YBCO-Cu piece with aluminum shell removed; (d) YBCO disk with copper disk removed; (e) measured mechanical strains in the half-moon shaped YBCO disk at different load steps. LS0 refers to the stress-free YBCO disk; LS1 refers to after shrink-fitting with the copper disk; LS2 refers to after shrink-fitting with the aluminum shell; LS3 refers to after compression by the copper disk at 77 K; LS4 refers to after compression by the aluminum shell at 77 K. The strain data for No.2 and No.8 are missing because of broken wires during the measurements.

(ii) Remove the aluminum shell from the YBCO-Cu-Al piece, as shown in figure 7(c), and record the balance values at RT as S_{YC}^{RT}, then immerse the YBCO-Cu piece and small YBCO block into LN_2 and record the measurement values as S_{YC}^{77K};

(iii) Remove the copper disk from the YBCO-Cu piece, as shown in figure 7(d), and record the balance values at RT as S_{Y}^{RT}, then immerse the YBCO disk and small YBCO block into LN_2 and record the measurement values as S_{Y}^{77K}.

Taking the final stress-free YBCO disk as the reference, the total measured mechanical strain, as shown in figure 7(e), consists of four contributions: (a) '$S_{YC}^{RT} - S_{Y}^{RT}$' due to shrink-fitting with the copper disk; (b) '$S_{YCA}^{RT} - S_{YC}^{RT}$' due to shrink-fitting with the aluminum shell; (c) '$S_{YC}^{77K} - S_{Y}^{77K}$' due to the compressive force provided by the copper disk upon cooling and (d) '$S_{YCA}^{77K} - S_{YC}^{77K}$' due to the compressive force provided by the aluminum shell upon cooling. The strain data for No. 2 and No. 8 are missing because of broken wires during the measurements. It can be observed from the plot that the major compressive strain comes from the compressive force provided by the copper disk when cooled to 77 K. Both shrink-fit assemblies contribute little to compressing the YBCO disk. Most of the compressive force provided by the aluminum shell at 77 K is absorbed by the copper disk and the residual force transmitted to the YBCO disk is limited. This suggests that the shrink-fit assembly with aluminum shell is not necessarily required in the bulk HTS undulator.

ORCID iDs

Kai Zhang https://orcid.org/0000-0002-3830-9682
Mark Ainslie https://orcid.org/0000-0003-0466-3680
John Durrell https://orcid.org/0000-0003-0712-3102
Marco Calvi https://orcid.org/0000-0002-2502-942X

References

[1] Casalbuoni S, Hagelstein M, Kostka B, Rossmanith R, Weisser M, Steffens E, Bernhard A, Wollmann D and Baumbach T 2006 *Phys. Rev. ST Accel. Beams* **9** 010702
[2] Ivanyushenkov Y 2017 *Phys. Rev. Accel. Beams* **20** 100701
[3] Kasa M *et al* 2020 *Phys. Rev. ST Accel. Beams* **23** 050701
[4] Halbach K 1983 *J. Phys. Colleq.* **44** 1–12
[5] Zhang K and Calvi M 2022 *Supercond. Sci. Technol.* **35** 093001
[6] Kesgin I *et al* 2021 *IEEE Trans. Appl. Supercond.* **31** 4100205
[7] Arbelaez D, Leitner M, Marks S, Mccombs K, Morsch M, Pan H, Prestemon S O, Seyler T and Schlueter R D 2018 *Synchrotron Radiat. News* **31** 9–13
[8] Boffo C 2010 Design and test of an HTS planar undulator prototype *Applied Superconductivity Conf.* (Washington, DC)
[9] Nguyen D N and Ashworth S P 2014 *IEEE Trans. Appl. Supercond.* **24** 4602805
[10] Kesgin I, Kasa M, Ivanyushenkov Y and Welp U 2017 *Supercond. Sci. Technol.* **30** 04LT01
[11] Holubek T, Casalbuoni S, Gerstl S, Glamann N, Grau A, Meuter C, Saez de Jauregui D, Nast R and Goldacker W 2017 *Supercond. Sci. Technol.* **30** 115002
[12] Kii T, Zen H, Okawachi N, Nakano M, Masuda K, Ohgaki H, Yoshikawa K and Yamazaki T 2006 *Proc. FEL2006 Conf., (Berlin, Germany)* pp 653–5
[13] Kinjo R, Shibata M, Kii T, Zen H, Masuda K, Nagasaki K and Ohgaki H 2013 *Appl. Phys. Express* **6** 042701
[14] Calvi M, Ainslie M D, Dennis A, Durrell J H, Hellmann S, Kittel C, Moseley D A, Schmidt T, Shi Y and Zhang K 2020 *Supercond. Sci. Technol.* **33** 014004

[15] Calvi M 2021 HTS undulators *Virtual Superconducting Undulators for Advanced Light Sources Workshop* (*21 April 2021*)
[16] Durrell J H *et al* 2014 *Supercond. Sci. Technol.* **27** 082001
[17] Huang K Y *et al* 2020 *Supercond. Sci. Technol.* **33** 02LT01
[18] Zhang K, Hellmann S, Calvi M, Schmidt T and Brouwer L 2021 *IEEE Trans. Appl. Supercond.* **31** 6800206
[19] Walker R P 1993 *Nucl. Instrum. Methods Phys. Res.* A **335** 328–37
[20] Krabbes G, Fuchs G, Canders W, May H and Palka R 2006 *High Temperature Superconductor Bulk Materials* (Weinheim: Wiley) pp 12–13 (available at: https://onlinelibrary.wiley.com/doi/10.1002/anie.200685418)